21 Analytical Techniques for Identifying Mineral Scales and Deposits

Valerie P. Woodward, Robert C. Williams, and Zahid Amjad

CONTENTS

21.1 INTRODUCTION

In many industrial processes, the feed water used contains mixtures of dissolved ions that are unstable with respect to precipitation. Various factors such as pH, temperature, the type and concentration of dissolved ions, flow velocity, equipment metallurgy, and so on contribute to the precipitation and deposition of sparingly soluble salts on equipment surfaces. The class of crystalline and amorphous compounds formed in industrial water systems, generically known as scale and deposits, has a widespread importance across a variety of disciplines, as can be seen from other chapters in this book and from other books [1–3]. *Scale* is defined as the deposit of certain sparingly soluble salts such as calcium carbonate, calcium phosphate, calcium oxalate, magnesium hydroxide, and calcium sulfate from the process fluids after precipitation onto the tubing and other process surfaces. The commonly encountered deposits in industrial water systems include carbonates, sulfates, and phosphates of alkaline earth metals, silica, magnesium silicate, corrosion products, microbiological mass, and suspended matter. These deposits, especially on heat-transfer surfaces in thermal distillation, cooling, and boiler systems, lead to overheating, loss of system efficiency, unscheduled shutdown, and untimely heat exchanger failure. In desalination by reverse osmosis (RO) process,

the deposition of unwanted precipitates may result in poor water quality and premature membrane failures. The deposition of scale in some cases may be beneficial as in the case of drinking water transmission lines wherein the layer of scale deposit protects the piping from corrosion by isolating it from the water. However, in most cases, scale is undesirable as it adversely affects the overall efficiency of the process.

Over the last three decades, considerable experience has been gained through the examination of failed heat exchangers and RO membranes; in that process, deposit characterization has been performed on the heat exchangers of different metallurgies and nearly every type of RO membranes, including spiral-wound, tubular, and hollow fiber configurations. In addition, the autopsies of the membranes of different compositions such as cellulose acetate, cellulose triacetate, and thin-film composite polyamide have been carried out using different analytical techniques for identifying the possible cause(s) of membrane failure and deposit composition. The information collected through deposit characterization has enabled the academic researchers and industrial technologists to develop new scale inhibitors, dispersants, and membrane cleaners. This chapter addresses the use of several analytical techniques to characterize the type, crystalline structure, and the composition of mineral scales and deposits. In addition, these techniques can also be used to identify the cause(s) of heat exchanger and membrane failures in the industrial water systems.

21.2 ANALYTICAL TECHNIQUES FOR IDENTIFYING MINERAL SCALES AND DEPOSITS

A number of methods may be employed to characterize mineral scales (i.e., calcium carbonate, calcium sulfate, barium sulfate, calcium fluoride, and so on) and deposits (i.e., rust, clay, zinc oxide, and so on). Some of these methods are listed in Table 21.1, along with the type of information and their advantages and disadvantages.

TABLE 21.1
Analytical Methods for Water Treatment Precipitates and Deposits

Technique	Information	Advantages	Disadvantages
Optical microscopy	M	Cost, time	Limited information
Scanning electron microscopy (SEM)	M, S	Time, sample size	Cost
Inductively coupled plasma	E	LDL	Sample size, prep time
Infrared	C	LDL, time, cost	Interpretation
Transmitted	C	LDL, time, sample size	Prep, sample must be homogenous
Reflected	C	Time, sample prep	Flat smooth surfaces, must be homogeneous
Energy dispersive x-ray spectrometry (EDS)	E	Time, sample size	LDL
X-ray photoelectron spectroscopy (XPS)	E, C	LDL, surface sensitivity, chemical states	Cost, interpretation
Wide angle x-ray diffraction (WAXD)	C	Time, phase identification	Cost, sample size
Particle size analysis (PS)	S	Time, cost	Size range limitations per instrument type, particles must stay suspended

Note: E, elemental; M, morphology; C, composition; S, size; LDL, lower detectable limit.

The following sections discuss various analytical techniques used to characterize commonly encountered scales and deposits. There is also a brief description of the other methods used in support of the deposit characterization, although it will not be as extensive as those listed above. These analytical techniques include:

- Optical microscopy
- Scanning electron microscopy and energy dispersive x-ray (SEM/EDS)
- Wide angle x-ray diffraction (WAXD)
- Particle size analysis
- Infrared spectroscopy

21.2.1 Optical Microscopy

Optical microscopy can be used to obtain color, size, crystalline structure, refractive index, and other information about water-formed deposits. The sample can be examined using a stereomicroscope or a compound optical microscope, both of which can have transmitted and reflected light sources. One of the most powerful tools in optical microscopy is polarized light illumination for particle classification. Many materials have distinct properties in polarized light—color, brightness, refractive index, and crystalline habits are only a few. These properties can be unique to specific materials and can serve as benchmarks for the experienced microscopist. Figures 21.1 and 21.2 illustrate the unique appearance of calcium carbonate and iron oxide. The brightness (birefringence) and high refractive index of calcium carbonate and the color of iron oxide are distinctive benchmarks that can guide the microscopist in identifying deposits.

Transmitted light observation can also be used to do microchemical spot tests to identify cations and anions if one does not have immediate access to SEM/EDS. A very common test for calcium carbonate is the addition of a droplet of 10% aqueous hydrochloric acid to a dry deposit sample to determine the presence of carbonate salts. The carbon dioxide evolution from carbonates occurs in the form of bubbles. Some disadvantages of optical microscopy include limited depth of focus, especially in reflected illumination, magnification limitations (~1 μm resolution), and lack of direct elemental information. When these limitations are encountered, SEM/EDS is the next step in the analytical scheme. Currently, most optical microscopes are equipped with digital cameras specifically designed for microscopic use. The cameras are accompanied by powerful capture and processing software, making acquisition, manipulation, storage, and usage of high-quality photomicrographs rather commonplace.

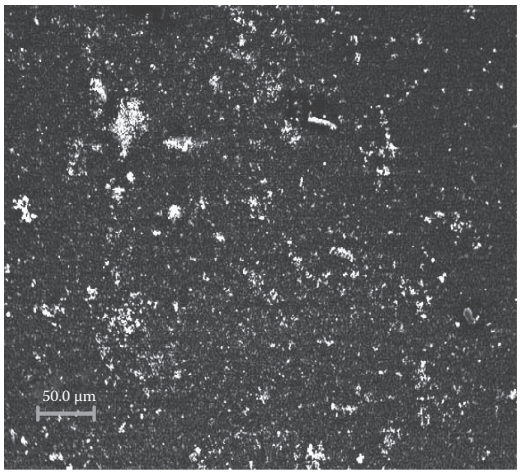

FIGURE 21.1 Transmitted polarized light micrograph of calcium carbonate (nominal 130×).

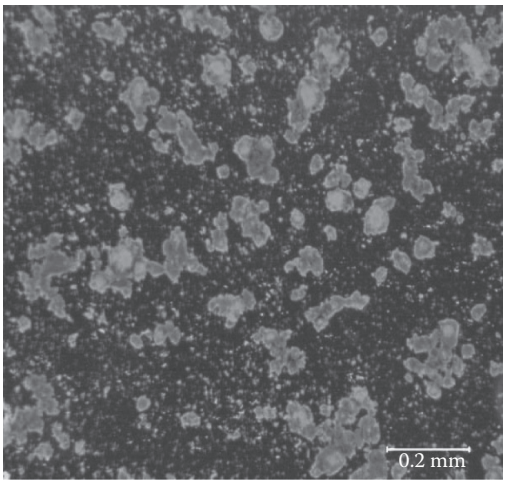

FIGURE 21.2 Transmitted polarized light micrograph of iron oxide (nominal 130×).

21.2.2 Scanning Electron Microscopy

The scanning electron microscope (SEM) is the next logical tool in the microscopy analysis scheme after optical microscopy. The SEM provides an excellent depth of field, a very large magnification range, several detection modes and flexible analysis environments, as well as a means to elemental analysis. Particle size, shape, crystal habits, packing tendencies, and the degree of agglomeration are all characteristics that can be elucidated via SEM imaging. A particularly informational usage of the SEM is tracking the morphology changes of mineral scale such as calcium carbonate. A series of standalone deposit particles or particles collected on filters during the laboratory evaluation of water treatment products can be compared for all of the previously noted attributes as well as for changes in particle population. Figures 21.3 and 21.4 are typical secondary electron images of Ca-containing deposits formed in the absence and presence of inhibitor.

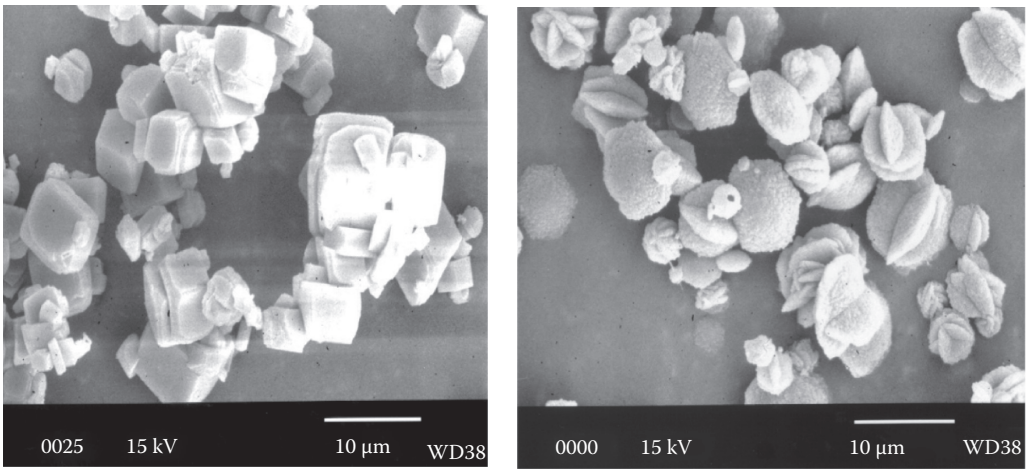

(a) (b)

FIGURE 21.3 SEM micrographs of two different calcium carbonate polymorphs; (a) vaterite and (b) calcite.

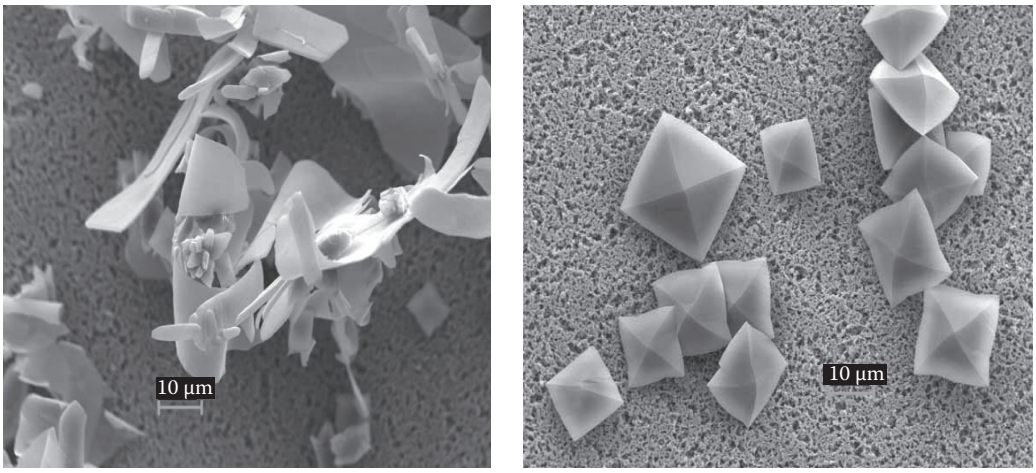

(a) (b)

FIGURE 21.4 SEM micrographs of calcium oxalate monohydrate (a) and calcium oxalate dihydrate (b) crystals formed in the absence and presence of inhibitor.

Figure 21.3a and b is an example of two different $CaCO_3$ polymorphs, namely, vaterite and calcite. Figure 21.4a and b shows the different morphologies of calcium oxalate crystals resulting from the absence or presence of an inhibitor. In the absence of an inhibitor, the crystals formed are calcium oxalate monohydrate ($CaC_2O_4{\cdot}H_2O$); however, the presence of 1 ppm Carbosperse™ K-732, a low-molecular-weight poly(acrylic acid), favors the formation of calcium oxalate dihydrate ($CaC_2O_4{\cdot}2H_2O$). Calcium oxalate scale, also known as "beerstone," is generally encountered in the brewing industry.

Current SEMs are entirely digital and allow the simple acquisition and storage of electronic images. Electronic image formats also allow ease of postprocessing, embedded annotation, and simple transfer to electronic documents. Another important aspect of the digital SEM is that the majority or all of the operations are performed via software. Until about 15 years ago, commercial SEMs were only available in the high-vacuum mode. High-vacuum SEMs required that the samples were dry and coated with a conductive metal or carbon to prevent charging (the poor conduction of the electron beam). Current SEMs are also available in high-pressure modes (also called variable pressure, low vacuum, and so on, depending on the manufacturer) and "environmental" modes (ability to image liquid water at room temperature). Both of these modes allow the analyst to observe uncoated samples or materials that are not completely dry.

SEM imaging and EDS elemental analysis are made possible by the interaction of a high-energy electron beam with a sample. Numerous types of interactions occur, mostly in the topmost 10 or so micrometers (μm) of a sample in 3D. The interactions of importance are those which allow the emission of secondary or backscattered electrons (imaging and atomic number contrast) and primary x-rays (elemental analysis). Most morphology imaging is performed in the secondary electron (SE) mode. The actual depth of penetration of the electron beam is dependent on the accelerating voltage of the electron beam and the atomic number of the specimen, with higher accelerating voltage and lower specimen atomic number yielding greater depth of penetration. The accelerating voltage relationship can be exploited to obtain surface information (lower voltage) or subsurface information (higher voltage). Secondary electron imaging can be performed in high-pressure modes as well as high vacuum with the advent of improved detectors made specifically for the collection of secondary electrons in the high-pressure environment. The majority of the images presented in this chapter were obtained between 15 and 25 kV accelerating voltage on metallized specimens in a high-vacuum mode.

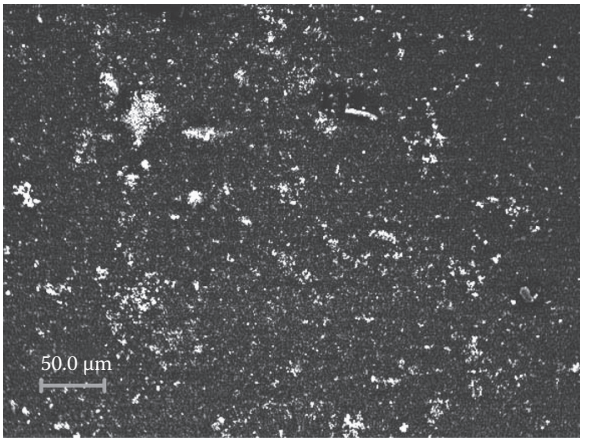

FIGURE 21.5 SEM micrograph in backscattered electron contrast (BSE) mode to facilitate locating small particles on filter substrate.

The backscattered electron (BSE) mode provides information from depths below that from which secondary electrons are generated and is sensitive to the average atomic number of the specimen if there is not much surface topography. BSE mode can be helpful in imaging samples that charge in high vacuum even when coated, and in locating higher atomic number particles on lower atomic number substrates. The former use of BSE is not so important if one has a high-pressure microscope. The latter method is extremely helpful when attempting to locate small particles in a low concentration on filters. Many times, the particles of interest and filtration debris cannot be distinguished from each other morphologically and can only be confirmed using energy dispersive x-ray spectrometry (EDS); however, performing EDS analysis on a number of tiny particles can be tedious. In the BSE mode, S-, Ca-, and Fe-containing particles will present themselves as brighter spots or areas on the darker filter background and make isolation for EDS analysis rather facile. Figure 21.5 illustrates typical BSE imaging of the mixed particles of calcium carbonate and iron oxide on a filter for the purpose of particle location. There are times when particle populations are quite sparse and manually searching the filter surface in the SE mode is time consuming. Using BSE to "light up" the particles that have significant average atomic number differences from the filter allow the analyst to go directly to a brighter spot and then spend quality analysis time to determine the particle morphology and elemental composition.

21.2.3 Energy Dispersive X-Ray Spectrometry Analysis

One of the more valuable assets of the scanning electron microscopy is the ability to obtain elemental composition information from materials. Characteristic x-rays from elements are generated at a depth below that from which backscattered electrons are generated; as in the imaging method, that depth can be affected by the accelerating voltage of the electron beam and the density of the specimen. EDS analysis can be used to obtain compositional information on quasi-bulk specimens (low SEM magnification and high accelerating voltage) or on specific particles, morphologies, or isolated areas on filters or within deposits.

Historically, detectors were protected from the SEM chamber environment with a thin window of beryllium, which limited the detection of elements to atomic number 10 (sodium) and above. Most current EDS detectors are able to detect boron, and in some cases beryllium, by the use of a thin polymer window between the chamber environment and the detector crystal. In addition to qualitative identification of the very low atomic number (low Z) elements, the thin window detectors also allow improved quantitative analysis of elements such as sodium and magnesium by virtue of

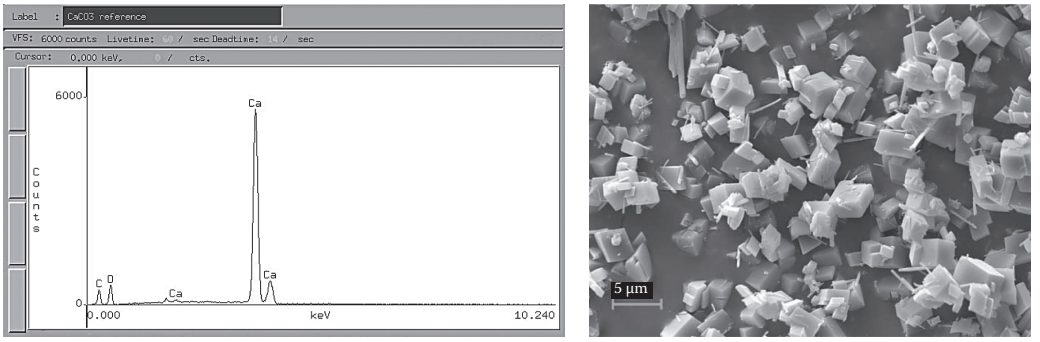

FIGURE 21.6 Typical EDS spectrum of calcium carbonate and SEM micrograph of sample from which EDS spectrum was generated.

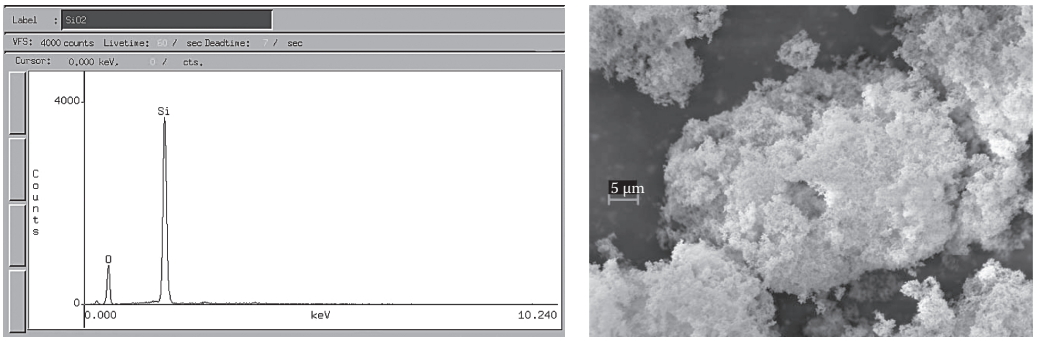

FIGURE 21.7 Typical EDS spectrum of silica and SEM micrograph of sample from which spectrum was generated.

improved signal-to-noise ratio in that area of the spectrum. Detection and quantification of lower atomic number elements can also be improved by the use of lower accelerating voltages, which confines excitation to elements in that range of energies. Figures 21.6 and 21.7 are typical EDS spectra and accompanying SEM images of $CaCO_3$ and SiO_2 collected with a thin window detector. Figure 21.6 illustrates $CaCO_3$ with a very crystalline morphology and its typical EDS spectrum at 20 kV accelerating voltage. Figure 21.7 illustrates an amorphous SiO_2 and its typical EDS spectrum. The ~200 nm primary particle size of the SiO_2 particles is the contributing factor to the amorphous nature of the material. In both EDS spectra, the peak intensity for oxygen is not intuitively as high as one would conjecture, considering that oxygen is ~48 wt.% of $CaCO_3$ and ~53 wt.% of SiO_2; however, the x-ray yield for very low-*Z* elements is low. If one were doing quantitative analysis, the algorithms used would take into account the x-ray line properties and the SEM conditions to correct for the low-*Z* yield.

Under certain conditions, EDS analysis can be quantitative as well as qualitative. For routine use, those conditions include homogeneous specimens, specimen thickness that is "infinite" to the beam penetration, relatively flat surfaces, and beam geometries that favor optimum collection of x-rays by the EDS detector. SEM column conditions are used by the EDS analysis programs in the correction algorithms; modern EDS analyzers can be integrated with digital SEMs so that information can be collected and stored automatically with the spectra; older instruments require the analyst to store the acquisition information manually with the spectra. There are also special conditions and programs that are required for quantitative analysis of individual particles, extremely small phases, and thin films, but those are not typically used in the characterization of water treatment precipitates and deposits.

21.2.4 Wide Angle X-Ray Diffraction

While EDS analysis in the SEM can provide elemental information about scales and/or deposits, there are times when it is necessary to know the form in which the materials exist. As an example, an EDS spectrum alone can indicate that there is C, O, and Ca in a deposit; however, it is necessary to know whether that is $CaCO_3$, CaO on carbon, or even an organic salt of Ca. WAXD of deposits, either removed from heat exchanger or RO membrane or on filters collected during precipitation experiments, provides crystalline phase information about those materials.

The theory of WAXD is based on the interactions of x-rays with the crystalline planes in materials. X-rays are generated. The resulting pattern takes the form of peaks of varying intensities, with the *x*-axis measured in either analysis angles (degrees 2θ) or *d*-spacing (Å) and the *y*-axis measured in counts per second. A typical crystalline low-background WAXD pattern for $CaSO_4 \cdot 2H_2O$ is shown in Figure 21.8, and a typical noncrystalline, mostly amorphous pattern, for silica is shown in Figure 21.9. A crystalline WAXD pattern, as illustrated in Figure 21.8, typically allows the analyst

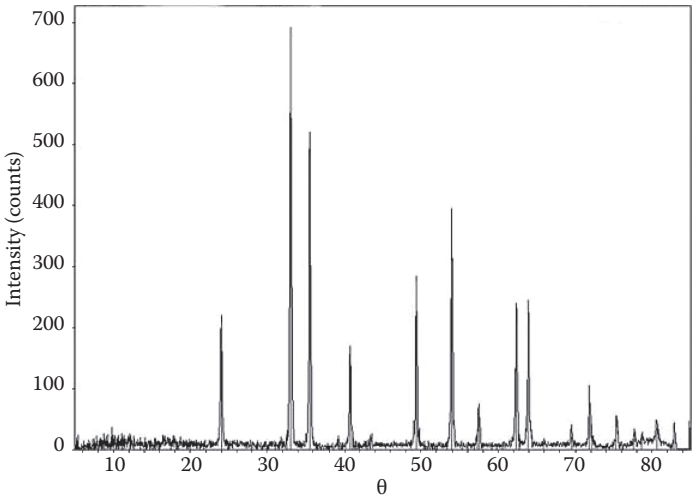

FIGURE 21.8 Low-background WAXD pattern of crystalline calcium sulfate.

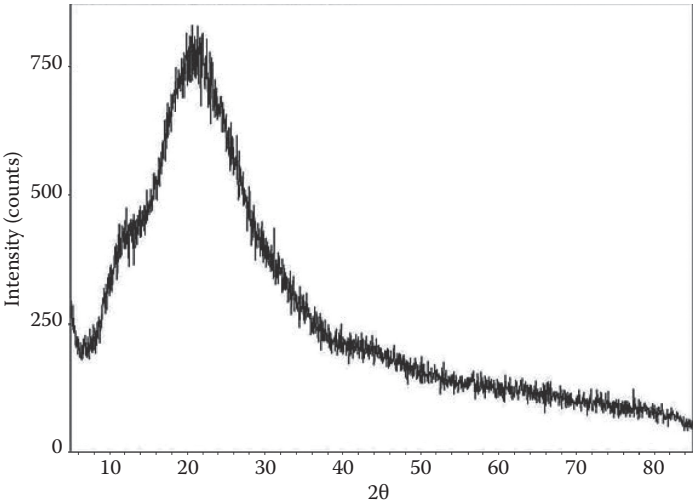

FIGURE 21.9 High-background WAXD pattern of amorphous silica.

to obtain a rather unambiguous identification of phase(s) using search-match programs with a high degree of certainty, given the pattern's well-formed reflections, excellent resolution, and low background. On the other hand, an amorphous pattern, such as that illustrated in Figure 21.9, makes phase identification nearly impossible; the best that can be achieved on this type of pattern is to determine the *d*-spacings of the approximate centroids of the broad reflections and to combine the EDS information with the *d*-spacings to manually search for sensible matches. The broad reflections can also be caused by very small (submicrometer) particle size; in this case, the material was the ~200 nm SiO_2.

Current WAXD acquisition is entirely computer-based and essentially automated. The sample preparation is the most labor-intensive portion of the analysis; if working with freestanding particles, they must be placed in the sample holder in a way that does not impart preferential orientation, and if working with particles on filters, the filters must be mounted in or on a holder in a way that does not change the sample height with respect to the incident x-rays. Preferred orientation can change a pattern such that it may not match known references, and the sample height above or below the incident beam level of the sample holder can lead to 2θ shifts in reflection positions. Both of these pattern changes can confuse the computer-based interpretation of the patterns and must be considered.

WAXD application programs are also completely computer-driven and their operations range from the basic marking of reflections to full quantitative analysis. Phase identification can be performed manually or automatically. Manual identification requires a general idea of phases that may be present in a material and the use of commercially available databases that one can search by chemistry, strongest reflections, phase name, and so on. Once reasonable candidates are identified, they can be visually applied to a pattern to check for fit. Automatic phase identification also uses the databases, but allows the analyst to tailor the searches for chemistry, statistical fit, preferred orientation, and many other aspects.

One of the more common applications of WAXD in the study of mineral scales and deposits is the determination of the polymorphs of $CaCO_3$. The polymorphs of most interest are the calcite, vaterite, and aragonite forms of the calcium carbonate. These forms have distinct WAXD patterns whose strongest reflections are well resolved from each other. Figure 21.10 illustrates a typical WAXD pattern of $CaCO_3$ with the different polymorphs indicated.

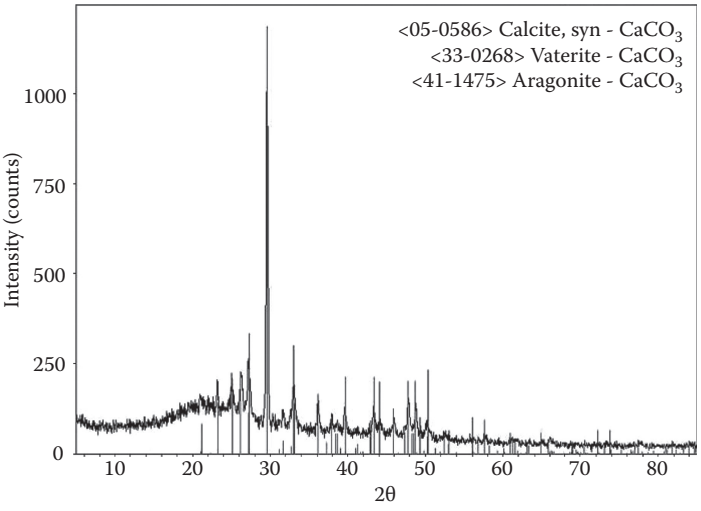

FIGURE 21.10 WAXD pattern of a mixture of calcium carbonate polymorphs—calcite, vaterite, and aragonite.

If deposits are directly on filters, it is important to acquire a reference pattern of an unadulterated filter under identical conditions to the deposits. The reference filter pattern can be used for qualitative comparison to (via overlays) or quantitative subtraction from the analysis patterns. A type of semiquantitative analysis of crystalline patterns can be accomplished if the phase identification is robust, the strongest reflections for those phases are well resolved from each other, and the background can be reasonably removed. For each element in the periodic table, mass absorption coefficients for various x-ray sources have been determined and are available in various reference tables. To determine the mass absorption coefficient of a compound, the elemental fractional composition of the compound is determined, each fraction is multiplied by the mass absorption coefficient for that particular element, and those products are summed to obtain the compound coefficient. The exercise for determining the mass absorption coefficient for $CaCO_3$ using Cu K-α radiation is illustrated as follows:

1. Determine weight fraction (*f*) of elements in $CaCO_3$:
   MW ($CaCO_3$) ≅ 100(1 mol Ca × 40 g/mol) + (1 mol C × 12 g/mol) + 3 mol O × 16 g/mol)
   Wt. fraction Ca ≅ 40/100 = 0.40
   Wt. fraction C ≅ 12/100 = 0.12
   Wt. fraction O ≅ 28/100 = 0.48
2. Mass absorption coefficients μ/ρ for elements Ca K-α (see note in optical microscopy microchemical tests section):
   μ/ρ Ca = 162
   μ/ρ C = 4.60
   μ/ρ O = 11.5
3. Mass absorption coefficient μ/ρ for compound $CaCO_3$ is shown in Table 21.2.

Once the mass absorption coefficients are determined for the compounds of interest, the next step in the semiquantitative analysis is to determine the net (background-subtracted) counts in the strongest reflections for each compound. The modeling of backgrounds and their subsequent subtraction and the determination of the net counts are reasonably facile procedures in current WAXD interpretation programs. Then, the net counts for each compound are multiplied by the mass absorption coefficient for the compounds and those products are summed. Finally, the individual products are divided by the sum and compositional fractions are obtained for a well-resolved, robust mix of $CaCO_3$, $CaSO_4$, and CaO, as illustrated in Table 21.3. If the pattern consists of the polymorphs of the same compound, there is no need to incorporate the mass absorption coefficients as they will be the same for each polymorph. In that case, a simple determination of the fractions based only on the net counts in the strongest reflection for each polymorph is indicated.

TABLE 21.2
Mass Absorption Coefficient μ/ρ Calculation for Compound $CaCO_3$

Element	Wt. Fraction (*f*)	μ/ρ	*f* × μ/ρ
Ca	0.40	162	64.80
C	0.12	4.60	0.55
O	0.48	11.5	5.52
Compound $CaCO_3$			70.87

TABLE 21.3
Determination of Approximate Phase Composition in a WAXD Pattern Using Net Areas under the 100% Reflections and Compound Mass Absorption Coefficients

Compound	μ/ρ (Rounded)	Net Counts	μ/ρ × Net Counts	~Fraction Compound
$CaCO_3$	71	15,000	1,065,000	0.3
$CaSO_4$	74	24,000	1,776,000	0.5
CaO	118	6,200	731,600	0.2
			3,572,600 (total)	

21.3 PARTICLE SIZE ANALYSIS

For particles deposited on filters or substrates, SEM or reflected light optical microscopy can be used to obtain various size measurements, including average size and size distribution. For the suspension of particles (i.e., calcium carbonate, iron oxide, and clay) in aqueous medium, automated particle analyzers are commonly used to provide many types of particle information. The modern analyzers are of several types, including x-ray sedimentation, electrical sensing zone, and laser light scattering. The particle size ranges and the analytical basis for each method are listed in Table 21.4.

Figure 21.11 illustrates the typical output from a laser light scattering instrument, with particle diameter on the *x*-axis and volume % on the *y*-axis. Figure 21.12 presents an excellent example of the particle size distribution of iron oxide in the absence and presence of a polymeric dispersant. As may be seen, the presence of 1 ppm Carbosperse™ K-781 exhibits a significant effect on the particle size distribution and causes a reduction of larger particles to smaller size particles. This type of information is useful in benchmarking the dispersants of different polymer architecture.

21.4 OTHER ANALYTICAL TECHNIQUES

Inductively coupled plasma, or ICP, analysis is a wet-chemical method for the quantitative determination of most metallic elements from the percent level to parts per trillion (ppt). This method requires that the sample can be taken up in a solution (some samples may require ashing and/or acid digestion) so that it can be aspirated into a plasma. The resulting atomic vapor emits light that is detected; the wavelengths are element-specific so that their intensities are proportional to the amount of analyte in the liquid sample. The method requires the analysis of the standard concentrations of the analytes in matrix-matched solutions to determine the response of the detection system. This method is particularly helpful when it is necessary to determine very low concentrations of metals in solutions from water treatments.

TABLE 21.4
Particle Size Analysis Ranges for Three Most Common Techniques

Technique	Particle Size Range (μm)	Theory
X-ray sedimentation	0.1–300	Natural size separation upon settling; mass fractions sensed by soft x-ray absorption
Electrical sensing zone	0.5–1000	Electrical signal proportional to volume of particles swept through an orifice; counts particles and determines concentration
Laser light scattering	0.02–2000	Mie and Fraunhofer theories to determine particle size distribution from a light-scattering pattern

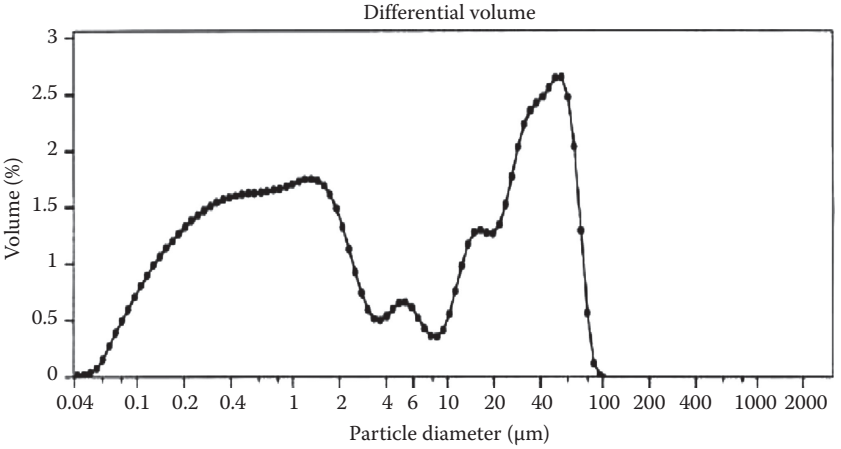

FIGURE 21.11 Typical output from laser light scattering particle size analyzer.

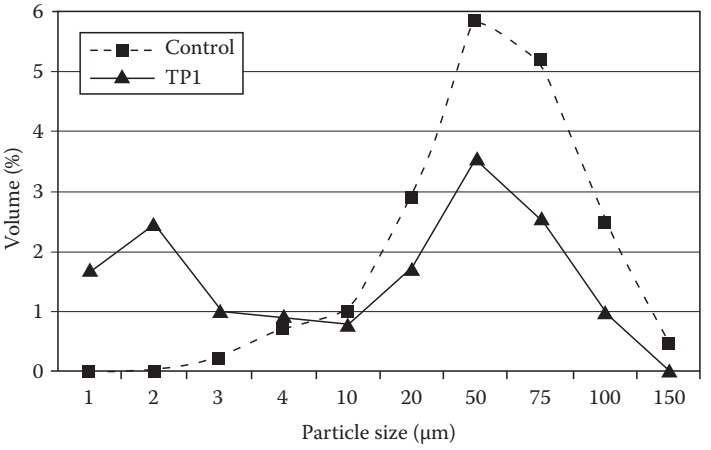

FIGURE 21.12 Comparison of particle size distributions of iron oxide in the absence and presence of Carbosperse™ K-781 terpolymer (TP1).

X-ray photoelectron spectroscopy, XPS (or colloquially ESCA, electron spectroscopy for chemical analysis), is a surface-sensitive elemental analysis technique. Electrons are ejected from inner or outer shells when excited by x-rays (the converse of EDS analysis, whence electron excitation causes ejection of x-rays). Each element has a specific binding energy that is affected by its atomic number and its coordination with other atoms. The position of the resulting peaks and their shifts from literature values aid the analyst in determining what analytes are present and if (and how) they are bonded to other atoms. XPS is sensitive to the first 10–50 Å of a surface and is particularly valuable when analyzing the thin deposits of the films of materials on substrates.

21.5 INFRARED SPECTROSCOPY

Infrared (IR) spectroscopy provides information that is complementary to the other methods that have been discussed. As the previous examples have illustrated, optical microscopy provides information on morphology, while ICP and the x-ray methods generally provide elemental information. However, with the exception of WAXD and XPS, none of these other methods provide any

information about chemical bonding or the specific chemical formula (although joint element mapping can sometimes provide some inferential information). Because IR spectroscopy usually detects bonds between atoms in a molecule, IR can often provide information regarding various functional groups in, and the chemical structure of, the analyte. However, just as the other methods have some limitations, so too does IR. Specifically, IR is the most sensitive to highly polar molecular bonds, is insensitive to nonpolar bonds between like atoms in diatomic molecules such as N_2, O_2, and Cl_2, and so on, and is relatively insensitive to molecular sulfur (S_8) and similar materials. Moreover, IR cannot usually detect materials based on purely ionic bonds, including many of the common, two-element salts, especially the common metal halides. Although a detailed discussion of the physics of IR and the associated instrumentation is beyond the scope of this chapter, the references include several works that do an excellent job of this [4–9].

However, the common IR limitations are really quite minute, when compared with the overall power of the method. IR can provide a "fingerprint" from pure materials, and a list of functional groups in mixture spectra from which the total composition can often be inferred. Moreover, the cost of a modern, benchtop IR is generally significantly lower than many of the SEM, x-ray, and ICP instruments; sample preparation issues are minimal; and results can be obtained very quickly. For these reasons, IR is often the first technique used, after initial microscopic screening, in the analysis of boiler scale deposits.

As was noted above, IR spectroscopy is complementary to the x-ray/ICP methods. In particular, IR is sensitive to and can usually identify organic components to which these other techniques are largely insensitive. In addition, it can often see the "other half" of some inorganic materials containing constituents to which the x-ray/ICP methods are blind. One such example is calcium carbonate, a commonly observed boiler scale material. Although the other methods can detect the calcium component, they are usually blind to the carbonate anion, and as was previously noted, even when all the elements are detected, it is still difficult to unambiguously determine the molecular formula. Conversely, the carbonate anion is unequivocally identified by IR, but this technique is relatively insensitive to the metal cation component, due to the ionic nature of the metal carbonate bond. The specific cation can often be inferred from the positions of several of the carbonate bands, but a confirming metals analysis is usually necessary for absolute certainty. In addition, because IR spectroscopy is sensitive to molecular bonds, it can often yield an indication of chemical changes in the analyte material, as will be shown in later examples. For the most part, these chemical changes might only be hinted at by changes in morphology in microscopic observation, and would not be detected at all by most x-ray and ICP methods.

The two most commonly used IR spectroscopic techniques in most laboratories are transmission spectroscopy and attenuated total reflectance (ATR) analysis [10–11]. (The latter is also sometimes referred to as frustrated multiple internal reflectance or FMIR.) The overlaid transmission and ATR spectra of calcium carbonate, plotted in absorbance mode, are shown in Figure 21.13. The pattern created by the three strongest peaks (i.e., the very strong, broad band in the region 1530–1320 cm^{-1}, accompanied by two weaker sharp bands in the regions 890–800 and 745–670 cm^{-1}) is diagnostic for carbonate anion; the specific cation can often be inferred from the exact positions of all the three bands [12]. Differences between these spectra will be explained in the ensuing discussions of these two techniques.

21.5.1 Transmission Spectroscopy

Transmission spectroscopy is an older technique, and was for many years by far the most commonly used infrared technique for a wide variety of samples. However, transmission spectroscopy also suffers from several disadvantages, especially when analyzing mineral scale and scale-inhibition materials. Aqueous media are difficult to analyze, both because many IR windows are water soluble and because it is difficult to prepare aqueous samples sufficiently thin for transmission spectroscopy. Similarly, solid samples need to be both relatively dry and very

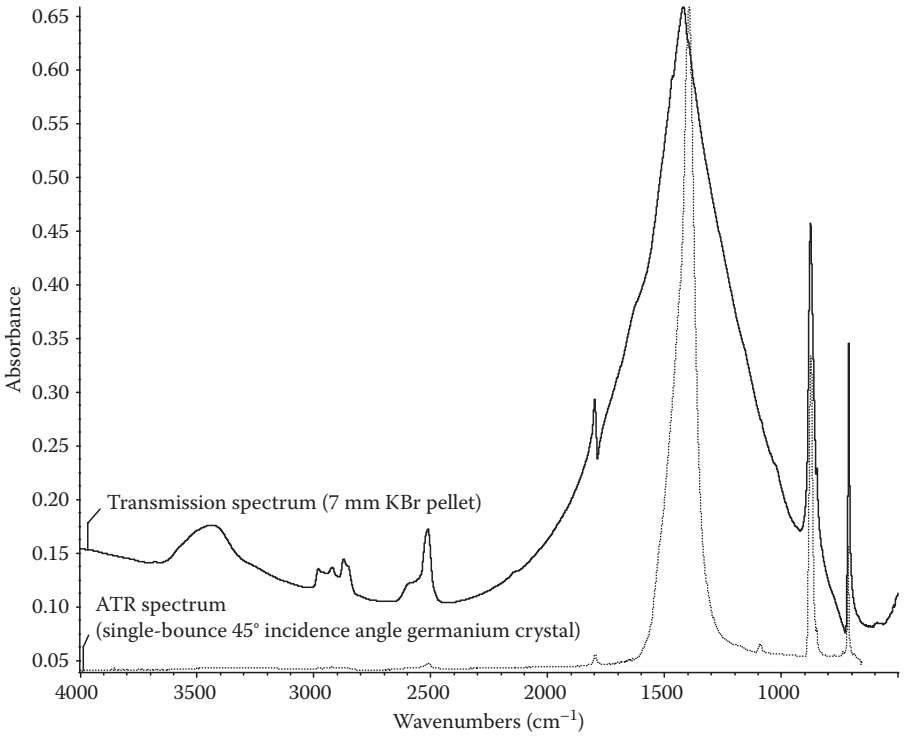

FIGURE 21.13 Infrared transmission and ATR spectra of calcium carbonate.

dilute in order to avoid exceeding the spectrometer's operating limits: typically approximately 10 microns thick for pressed polymer or cast organic films, and sometimes less for inorganic materials. Solid samples that can neither be pressed nor dissolved are commonly prepared either as very dilute (typically less than 1 wt.%) suspensions in a pressed potassium bromide pellet matrix or as dispersions in Nujol® mineral oil. The IR transmission spectrum of calcium carbonate, shown in Figure 21.13, was acquired as a KBr pellet. Unfortunately, this technique can be moderately labor intensive and is not suitable for aqueous liquids or wet solids. In addition, the interaction of the analyte material with the KBr-pelletizing matrix can cause band frequency shifts and other artifacts, including occasional spurious bands. The mineral oil dispersion technique is no longer commonly used, since it has been superseded by other newer techniques, including ATR.

Another application of transmission spectroscopy is the use of an IR microscope (which, in many instances can also acquire reflectance and micro-ATR, as well as transmission spectra) [13]. This application is best suited for heterogeneous samples, where several compositionally different (but preferably, spatially separated) materials are present on the same substrate, and/or for very small samples, where there is insufficient material to use one of the other techniques. However as in the case of ordinary transmission spectroscopy, there is an upper limit on the sample thickness that can be analyzed using transmission IR microscopy. In addition, it can be difficult to sort out all the constituents in a heterogeneous sample. Ideally, for transmission IR microscopy, each of the individual particles should be homogeneous, but there can be different spatially dispersed particle species present; for ATR, it is desirable that all of the particles be compositionally similar (although it is sometimes possible to obtain useful information when several different particle species are present). For most of the applications in our laboratory, the samples were sufficiently homogeneous (and sufficiently large) that macro-ATR was a more appropriate choice.

21.5.2 ATR-IR Spectroscopy

In contrast to the various transmission techniques, ATR spectra can be collected very quickly for a wide variety of liquid and solid samples with essentially no sample preparation. In addition, the accessories now in use are capable of analyzing samples as small as 300 microns in diameter. While this is still considerably larger than the lower limit for a good IR microscope (around 10–20 microns), it is often sufficient for a wide variety of samples. Moreover, the cost of a good ATR unit can be one-tenth or less than the cost of a good IR microscope. These advantages generally render ATR more appropriate as the first-choice approach for the initial screening of boiler scale and water treatment samples.

ATR-IR spectroscopy is normally presented by invoking quantum mechanical tunneling [10]; however, an alternate conceptual approach which does not require any knowledge of or familiarity with quantum mechanics is presented here. Visual information associated with this explanation is shown in Figure 21.14. The physics associated with the ATR technique is the same one involved when a person underwater in a swimming pool looks up out of the water. If the swimmer looks straight up, he or she will see the ceiling of the swimming pool. However, if that same swimmer begins to look toward the end of the pool, at some point, instead of seeing the ceiling, he/she will see the floor at the far end of the swimming pool. This is a practical illustration of *Snell's law*. When a light ray in an optically dense medium (in this case, water) strikes an interface between that medium and a less optically dense medium (in this case, air) at any angle other than zero degrees (i.e., perpendicular to the interface), it will normally be refracted away from the perpendicular. As the angle of incidence increases from zero, at some point, it will reach a critical angle, beyond which the incident ray is *totally internally reflected* back into the denser medium. This critical angle is defined by the two indices of refraction and can be calculated using Snell's law. Although there may be some reflective loss, rays striking the interface at less than the critical angle (i.e., more nearly perpendicular to the interface) will always be at least partially transmitted; however, rays striking the interface at anything greater than the critical angle (i.e., more nearly parallel to the interface) will always be totally internally reflected.

Now, replace water in the example above with a high-index material such as germanium, zinc selenide, or diamond, and replace the air with a water treatment sample. Suppose that there is some means of monitoring the internally reflected ray, and consider a ray that is incident at a value very close to, but slightly greater than, the critical angle. It has already been stated that this ray is normally totally internally reflected. Now, examine what happens if that rarer medium is a material that has an absorption band occurring at the same energy as the incident ray. Around a strong absorption

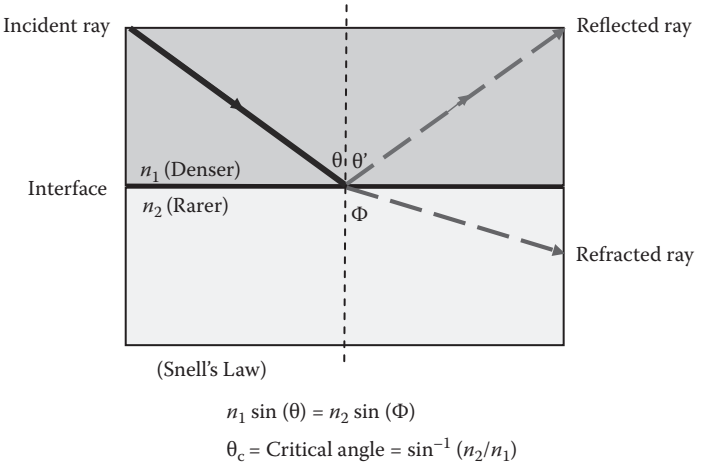

FIGURE 21.14 Schematic illustrating principles underlying the ATR technique.

band, the index of refraction increases drastically. This increased index of refraction means that in the region of this absorption band, there is now a different critical angle, which is greater than the absorption-free critical angle. If conditions have been chosen appropriately, the net effect is that the incoming ray is now incident at *less than* the new critical angle, and that there will be at least some transmission from the denser to the rarer medium. The ray that was formerly totally internally reflected is now said to be *attenuated* by the portion that was transmitted. If an infrared spectrometer is used to scan the spectral range and to measure the intensity of the internally reflected refracted ray, the result is a spectrum that is qualitatively similar to the conventional transmission spectrum of the rarer medium. The effective sampling depth of this technique (which can be calculated using quantum mechanics) is dependent on the denser medium and analyte indices of refraction and varies as a function of the incident wavelength, but is typically on the order of a few microns. The effective penetration depths for several commonly used crystal materials at a variety of incidence angles are shown in Table 21.5.

To some extent, the effective sampling depth at any given wavelength can be altered either by adjusting the angle of incidence and/or by choosing an alternate substrate medium that has a different optical density. There have been papers on "spectroscopic microtoming," where successively deeper penetration depths would sometimes reveal layers below the surface [11,14]; however, in more recent times, this technique has essentially been superseded by the IR microscopic analysis of sample cross sections.

As previously noted, one of the major advantages of ATR is the minimal sample preparation involved. Figure 21.15 is a schematic of one commonly used ATR configuration. This is a single-bounce unit that utilizes a 45° incidence angle; the crystal material can be germanium ($n = 4$), zinc selenide, or diamond ($n \sim 2.4$ for both). Because the working surface of the ATR crystal is less than 1 mm in diameter, only minimal sample quantities are required. Acceptable spectra have been acquired from sample spot sizes as small as 0.3 mm in diameter. For solid samples (including deposits on filter paper), it is merely necessary to use some form of clamp to press the sample into intimate contact with the ATR crystal. (Best results are obtained if the surfaces are flat and moderately smooth; good results have also been obtained for many powders.) Liquid samples can be run neat, in a sample cup. Wet solids can be run as received, although better results can usually be achieved if the sample is dried first; otherwise, the strong water bands will often obscure some of the analyte bands of interest. In addition, this technique is nondestructive; analyzed samples can usually be recovered for use in subsequent tests.

Because the ATR method interrogates only the first several microns of the material in contact with the crystal, it is ideally suited for the analysis of coatings as well as material deposited on the surface of filter media (although it is sometimes necessary to digitally subtract the spectrum of the filter substrate). However, the surface sensitivity of ATR is significantly worse than what can be achieved with SEM-EDS.

TABLE 21.5
Effective Penetration Depth (Microns) into a 1.50 Index Medium

Crystal	Incidence Angle	Wave Numbers (cm^{-1}) 3000	2000	1000	500
Ge	30	0.40	0.60	1.20	2.40
Ge	45	0.22	0.33	0.66	1.33
Ge	60	0.17	0.25	0.51	1.02
ZnSe and diamond	45	0.67	1.00	2.00	4.00
ZnSe and diamond	60	0.37	0.55	1.11	2.21

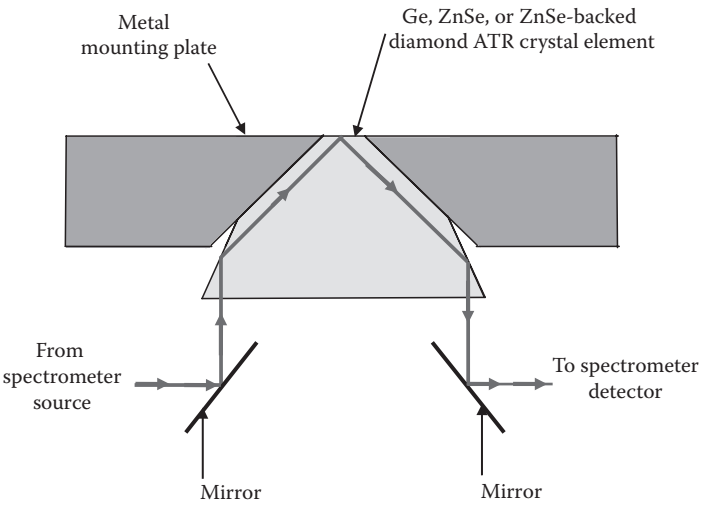

FIGURE 21.15 Generalized schematic of a single-bounce ATR accessory.

One of the primary limitations of the ATR technique is the necessity of good surface contact between the analyte and the crystal window in order to obtain an acceptable spectrum. Although this issue has been minimized by the advent of ATR accessories that utilize much smaller contact areas, badly abraded or etched surfaces or very coarse powders may not yield sufficiently good contact to acquire useful spectra. However, the flatness required is still significantly less than that necessary for backscattered SEM imaging.

Other limitations are dictated by the basic physics inherent in this technique. Because the effective sampling depth (and hence, apparent sample thickness) is a function of wavelength, ATR spectra show diminished band intensities in the high-frequency region, and enhanced intensities in the low-frequency region, relative to what is observed in a normal transmission spectrum. The peak frequency values can also shift by up to 20 (but usually less than 10) cm^{-1}, relative to the transmission values, but often will not shift at all. Some of these differences are illustrated by the calcium carbonate transmission and ATR spectra overlaid in Figure 21.13. ATR-induced artifacts can also make searching an ATR spectrum against transmission libraries problematic; however, several instrument companies now provide proprietary software that does a relatively good job of converting an ATR spectrum to a "pseudotransmission" spectrum in order to facilitate such searches.

Another potential issue with the ATR technique is that very thin (less than 0.5 micron thick) coatings may not be detected, especially if there are no strong coating bands in the high-frequency portion of the spectrum, where the penetration depth is smallest. Moreover, it must always be remembered that ATR is a surface technique that may not accurately reflect the composition of materials below the surface. Finally, as in the case of transmission spectroscopy, in a complex mixture, it may be difficult to completely characterize all of the constituents; however, the technique can be quite useful for simple mixtures, especially ones that are primarily inorganic.

21.6 APPLICATIONS TO WATER-TREATMENT PROBLEMS

21.6.1 Metal-Inhibitor Salt Formation

Scale inhibitors (polymeric and nonpolymeric) used in water treatment formulations may form insoluble salts with metal ions (e.g., Fe, Ca, Ba, and Sr) under conditions frequently encountered in cooling water systems. The trend toward the operation of cooling water systems under increasingly severe operating conditions (e.g., high hardness, high alkalinity, and increased pH and temperature) has favored the formation of insoluble calcium-inhibitor salt. For this reason, the metal ion tolerance

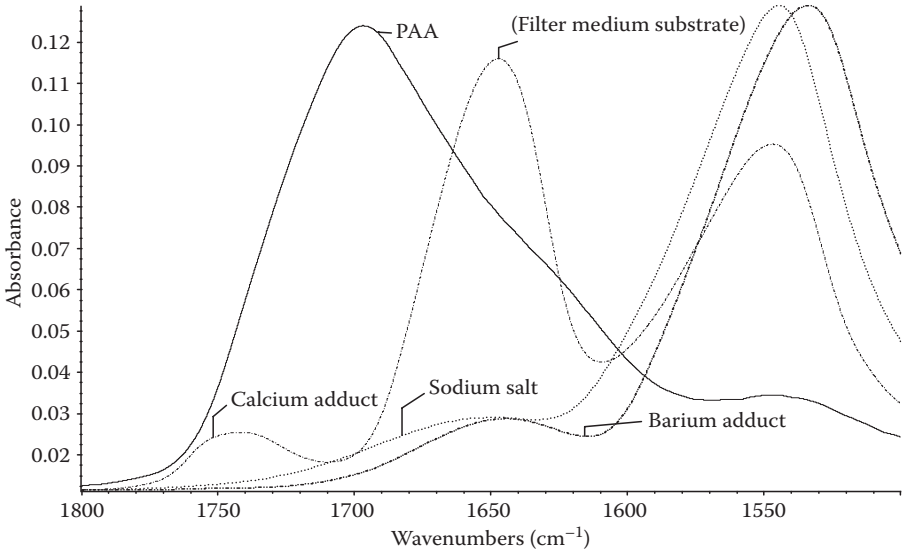

FIGURE 21.16 IR spectra of PAA and several metal salts. All salts were vacuum-dried. PAA and sodium salt spectra were acquired from neat powders. Calcium and barium adducts were on filter media. The band near 1647 cm^{-1} on the calcium adduct spectrum is from the underlying filter medium.

or the ability of the inhibitor to remain soluble in the presence of metal ions is of increasing importance. The precipitation of metal-inhibitor salt on heat exchanger and RO membrane surfaces lead to poor system performance. A typical application of ATR to metal–polymer scaling problem is shown in Figure 21.16 [15]. In this figure, the diamond ATR spectra of poly(acrylic acid) (PAA), a common boiler scale inhibitor, and its sodium, calcium, and barium salts are shown in the 1800–1500 cm^{-1} region. In this case, the PAA and its sodium salt were supplied as aqueous solutions, which were vacuum-dried, following which the spectra of the dried powders were acquired. The calcium and barium precipitates were isolated on a 0.22 micron cellulose nitrate filter, and then vacuum-dried. Spectra were acquired directly from the filter, with no subtraction or other correction. For the barium precipitate, coverage was sufficiently complete that most of the filter bands are masked by the barium salt. For the calcium salt, however, there was apparently less material on the filter, and the underlying cellulose nitrate band near 1650 cm^{-1} is evident. In Figure 21.16, the chemical change occurring as the acid is converted to salt is clearly evident with the loss of the acid carbonyl band near 1700 cm^{-1}, and the corresponding growth of the carboxylate salt carbonyl band near 1547, 1543, and 1533 cm^{-1}, respectively, for the calcium, sodium, and barium salts. Note that the calcium and sodium salt bands occur at almost the same frequency. Moreover, it is also known that these frequencies can vary slightly as a function of concentration, and the calcium salt precipitate is known to be a relatively diffuse coating on the filter medium. If these samples had not been lab specimens whose compositions were well known, this would be an example of the possible need for x-ray/ICP analysis to distinguish between two possible cation possibilities. Further discussion on metal-inhibitor salts is presented in Chapter 5.

21.6.2 Cationic Polymer-Anionic Polymer Coacervate Formation

As discussed in Chapter 5, the role of anionic polymers such as PAA in water treatment formulations is to prevent the precipitation of mineral scaling salts such as calcium carbonate and calcium sulfate. Cationic polymers such as diallyldimethyl ammonium chloride (*p*-DADMAC) and copolymers of acrylic acid:acrylamide are commonly used as flocculating agents to help in removing suspended and colloidal matter from the feed water. It has been reported that the low levels (<1 ppm)

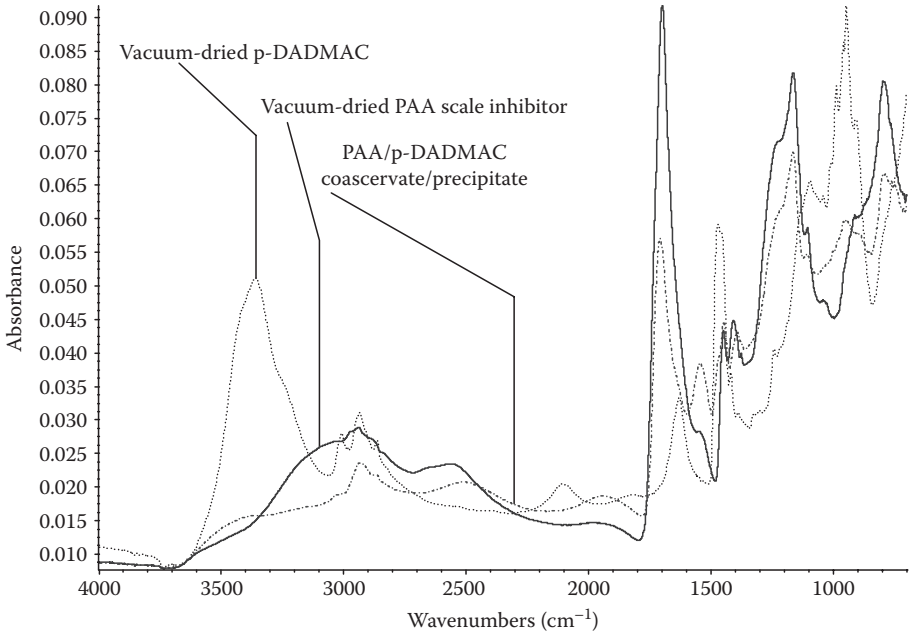

FIGURE 21.17 IR spectra of PAA/*p*-DADMAC coacervate/precipitate.

of cationic polymer interferes with the performance of anionic polymer used in the water treatment formulation. A second ATR application example is shown in Figure 21.17, in this instance using a zinc selenide crystal. These spectra come from a study of anionic polymer-cationic polymer coacervate precipitation. In this instance, an approximately 5000-MW PAA was mixed with *p*-DADMAC. The overlaid spectra (all of vacuum-dried materials) include the PAA, the *p*-DADMAC, and the coacervate precipitate resulting from the mixture of the concentrated solutions of the first two ingredients. Although the bands attributable to the PAA dominate the precipitate spectrum (albeit with some small frequency shifts), the shoulders near 3400, 1470, and 950 cm^{-1} suggest the presence of the *p*-DADMAC salt, and correspond roughly to bands seen in the neat *p*-DADMAC spectrum. These data were used to confirm a hypothesis developed during the turbidity studies of PAA-*p*-DADMAC solutions. Additional information on polymer–polymer interaction is presented in Chapter 5.

21.6.3 Thermal Treatment of Deposit Control Polymers

Figures 21.18 and 21.19 present the results from several time-temperature stability studies of 10% solutions of PAA and some common co- and terpolymer constituents [16]. The spectra of the actual solutions (not shown) consisted mainly of water-solvent bands which masked out the information of interest. In order to avoid inducing any additional thermal history to the heat-aged samples, several drops of solution were deposited in the ATR liquid sample cup, and dried with an impinging room-temperature nitrogen stream for in excess of 10 min. The spectra of the residues remaining after drying were acquired using a germanium ATR crystal.

Figure 21.18 shows the spectra of a terpolymer of acrylic acid:2-acrylamido-2-methylpropane sulfonic acid:sulfonated styrene (AA:AMPS®:SS) monomer both before thermal treatment and after two different treatment times. (In order to avoid interference from residual water bands, these solutions used 99% pure deuterium oxide, rather than normal water.) The heat-aged sample spectra are quite similar; however, both exhibit significant differences from the original untreated PAA:AMPS:SS terpolymer, especially in the intensities of the bands near 1649 (amide carbonyl),

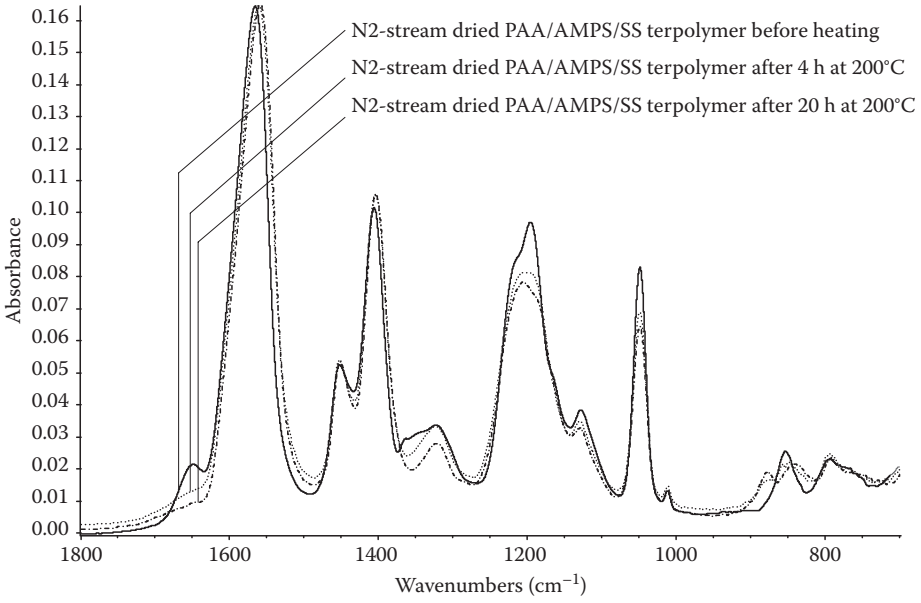

FIGURE 21.18 PAA/AMPS/SS terpolymer with and without heat treatment.

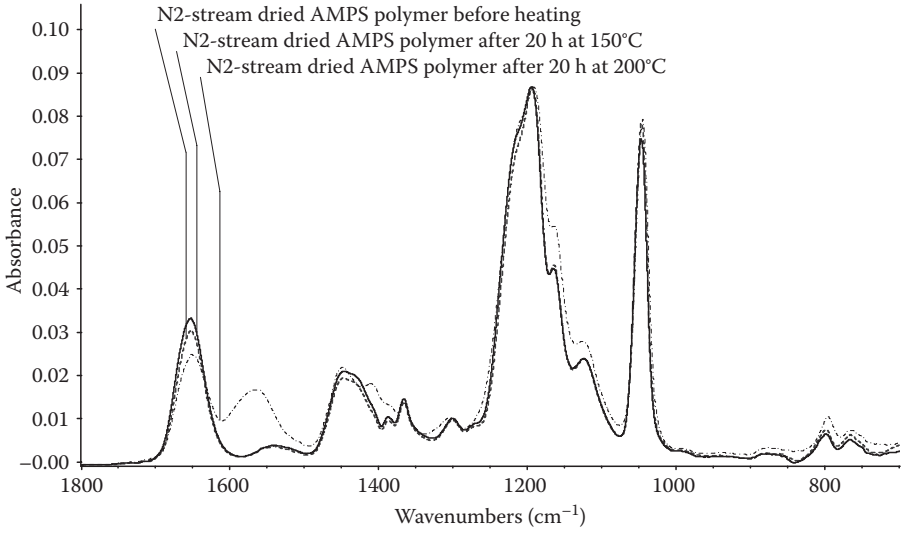

FIGURE 21.19 IR spectra of poly-AMPS with and without heat treatment.

1196 (asymmetric SO_3 stretch), and 1049 cm^{-1} (symmetric SO_3 stretch) and to a lesser extent, the band near 1405 cm^{-1} (asymmetric SO_2 stretch); in addition, there are small band shifts in three of these bands. The disappearance of the 1649 cm^{-1} correlates well with the expected loss of amide carbonyl band as this moiety is oxidized; the other differences are ascribed primarily to a suspected pH shift and other changes in molecular geometry caused by the degradation of the AMPS component. In any event, the similarity of the 4 and 20 h traces indicates that most of the decomposition in this formulation occurs within the first 4 h.

Figure 21.19 contains the spectra of poly-AMPS before heat treatment and after 20 h heat treatment at 150°C and 200°C, respectively. Although there are some small differences between the unheated

and 150°C spectra, they are quite similar; however, the 200°C spectrum differs significantly. These results suggest that poly-AMPS is relatively stable at 150°C, but degrades readily at 200°C.

The spectra shown in these examples represent a few of the IR analyses we have performed to obtain information on chemical changes that can occur to boiler water treatment chemicals due to precipitation with hard water cations or cationic polymers and during prolonged exposure at elevated temperatures. The results of these studies have been and will be used to design more stable and more effective water treatment packages.

21.7 SUMMARY

A variety of analytical techniques are available to analyze complex mineral scales and deposits commonly encountered in industrial water systems. In selecting a method of analysis, the important roles played by various microscopic methods, EDS, and WAXD, in identifying composition, crystalline structure, and crystal morphology of foulants should be considered. The utility of particle size analysis in studying changes in the particle size of foulants such as iron oxide, clay, calcium carbonate, and so on (especially in the presence of deposit control polymers) must also be kept in mind. In addition, IR spectroscopy is an excellent tool for detecting chemical changes in polymer architecture under conditions typically encountered in industrial water systems.

REFERENCES

1. Amjad, Z. *Reverse Osmosis: Membrane Technology, Water Chemistry, and Applications,* Van Nostrand Reinhold, New York (1993).
2. Schroeder, C. D. *Solutions to Boiler and Cooling Water Problems*, The Fairmont Press, Inc., Atlanta, GA (1986).
3. Cowan, J. C. and Weintritt, D. J. *Water-Formed Scale Deposits*, Gulf Publishing Company, Houston, TX (1976).
4. Colthup, N. B., Lawrence, H. D., and Wiberly, S. E. *Introduction to Infrared and Raman Spectroscopy*, 3rd edn., Academic Press, New York (1990).
5. Smith, B. *Infrared Spectral Interpretation*, CRC Press, Boca Raton, FL (1999).
6. Silverstein, R. M., Francis X. W., and Kiemle, D. *Spectrometric Identification of Organic Compounds*, 7th edn., Wiley, New York (2005).
7. Socrates, G. H. *Infrared and Raman Characteristic Group Frequencies: Tables and Charts*, 3rd edn., John Wiley & Sons, New York (2001).
8. Smith, B. *Fourier Transform Infrared Spectroscopy*, CRC Press, Boca Raton, FL (1996).
9. Griffiths, P. R. and de Haseth, J. A. *Fourier Transform Infrared Spectrometry*, 2nd edn., Wiley-Interscience, New York (2007).
10. Harrick, N. J. *Internal Reflection Spectroscopy*, Wiley-Interscience, New York (1967).
11 Urban, M. W. *Attenuated Total Reflectance Spectroscopy of Polymers: Theory and Practice*, American Chemical Society, Washington, DC (1996).
12. Nyquist, R. A. and Kagel, R. O. *Infrared Spectra of Inorganic Compounds*, Academic Press, New York (1971).
13. Messerschmidt, R. G. and Harthcock, M. A. (Eds). *Infrared Microspectroscopy: Theory and Applications*, Marcel Dekker, New York (1988).
14. Hirshfeld, T. Subsurface layer studies by attenuated total reflection Fourier transform spectroscopy. *Appl Spectrosc* 31(4), 239–292 (1977).
15. Amjad, Z. Interactions of hardness ions with polymeric scale inhibitors in aqueous systems. *Tens Surf Deterg* 42, 71–77 (2005).
16. Amjad, Z. and Zuhl, R. W. The impact of thermal stability on the performance of polymeric dispersants for boiler water systems. In: Paper presented at the Association of Water Technologies, Inc. Annual Convention, Palm Springs, CA (2005).